35th Annual International Conference of the IEEE EMBS
Osaka, Japan, 3 - 7 July, 2013

Light-Induced Microbubble Poration of Localized Cells

Qihui Fan, *Student Member, IEEE*, Wenqi Hu, *Student Member, IEEE*,
and Aaron T. Ohta, *Member, IEEE*

***Abstract*— Molecular delivery into localized NIH/3T3 cells was achieved with microbubbles produced by laser pulses focused on an optically absorbent substrate. The laser-induced bubble expansion and contraction resulted in cell poration. The microbubbles are localized at the laser focal point, so molecular delivery can be directed at specific localized cells. This was demonstrated with the delivery of 3-kDa FITC-Dextran. Single-cell molecular delivery was achieved, even in the presence of nearby cells. The efficiency of the cell poration was up to 95%, with a corresponding cell viability of 98%.**

I. Introduction

Transferring exogenous molecules into specific cells at localized spatial locations is a challenge in cell biology, as widely used molecular delivery technologies are based on treating large amounts of cells simultaneously. Nevertheless, the ability to target cells for molecular delivery is helpful in many cases, such as stem cell research and other situations where cell modification needs to be induced on site [1]. Viruses or chemical complexes are widely used to transfer molecules into cells, but they are not suitable for targeting cells at specific spatial locations [2]. Another molecular delivery method is electroporation [3], which uses pulsed electric fields to open pores in the cell membrane. However, the electroporation of localized cells is a serial operation, limiting throughput [4, 5]. Optically induced electroporation enables parallel operation due to the incorporation of multiple light-induced virtual microelectrodes, which increases throughput, but with some restrictions on the type of media [6]. In contrast, sonoporation uses acoustic energy facilitated by microbubbles to porate cells [9, 10]. However, sonoporation is currently unable to transfer molecules into localized cells [11, 12]. Microinjectors can achieve high-efficiency molecular delivery to localized cells, although this is also a serial operation [7, 8].

Molecular delivery using nanosecond to femtosecond laser pulses is promising for localized cell poration [13-15]. A 6-ns laser pulse can induce cavitation bubbles that porate nearby cells, although more optimization is needed to avoid lysis of neighboring cells [13]. Femtosecond laser-induced poration can achieve high spatial precision, but the efficiency of the delivery still has room for improvement [16, 17]. It is desirable to retain the flexibility and specificity of the laser-based poration, while increasing the efficiency of the molecular delivery.

Lasers can also control the generation of microbubbles in saline media [18]. These microbubbles can be used for localized cell poration, as their position and size can be controlled precisely. Here we report on a method that uses laser-induced microbubbles to porate spatially localized single cells, enabling molecular delivery. To achieve poration, a pulsed laser is focused onto an optically absorbing surface near the edge of a cell (Fig. 1a). When the laser is on, the heat from the optical absorption produces an expanding microbubble (Fig. 1b). When the laser pulse is off, the bubble collapses. The process repeats during subsequent pulses, causing bubble oscillation and induced microstreaming around the microbubble (Fig. 1c). This creates shear stress on the cell membrane, resulting in laser-induced microbubble poration (LMP). Exogenous molecules transfer into cell interiors via the induced pores in the cell membrane. Once the laser pulses cease, the microbubbles stop oscillating, and the pores reseal, restoring the membrane (Fig. 1d).

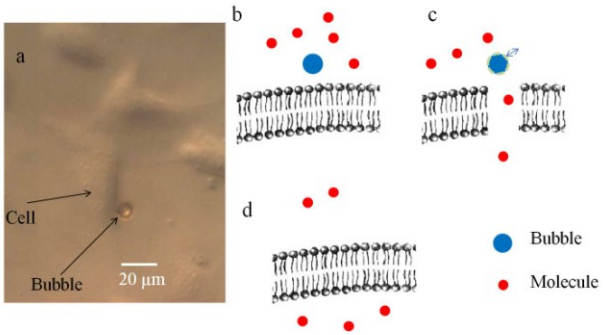

Figure 1. The mechanism for the poration of cells via laser-induced microbubbles. (a) A laser-induced microbubble interacts with NIH/3T3 cells. (b) A laser pulse produces a microbubble near the cell membrane. (c) As the laser pulses continue, the bubble collapses and expands, causing pores to open in the cell membrane. Molecules can travel into the cell interior. (d) When the laser pulses cease, the cell membrane reseals.

LMP provides an efficient poration method for single adherent cells. Compared to other laser-based cell poration systems, this method can achieve high selectivity while keeping the processed cells from direct laser illumination. Further, LMP works with a variety of liquids, including many cell culture media and saline buffer solutions.

II. Poration System

The LMP functions through the interaction between the oscillating microbubble and the target cell's membrane. Previous reports observed that molecular delivery occurred

This work was supported by Grant Number 1R01EB016458-01 from the National Institute of Biomedical Imaging and Bioengineering of the National Institutes of Health (NIH). These contents are solely the responsibility of the authors and do not necessarily represent the official views of the NIH.

Q. Fan is with the Department of Mechanical Engineering at the University of Hawai'i at Mānoa, Honolulu, HI 96822 USA (phone: 808-956-8196; fax: 808-956-3427; e-mail: fanqihui@hawaii.edu).

W. Hu and A. T. Ohta are with the Department of Electrical Engineering at the University of Hawai'i at Mānoa, Honolulu, HI 96822 USA (emails: wenqihu@hawaii.edu, aohta@hawaii.edu)

when the cell had a certain deformation [11]. In this LMP system, the primary factor for the cell deformation and subsequent poration is the dynamic shear stress produced by the cavitation bubble expansion [13, 19]. The maximum shear stress rapidly reduces as the distance from the microbubble increases [13]. There is an optimum shear stress to induce cell poration: when the shear stress is very strong, it can cause cell lysis, but if the shear stress is too weak, there may not be sufficient poration for efficient molecular delivery. The system in this report can produce controllable and reproducible microbubbles, and can position the microbubbles at desired locations to achieve the optimum shear stress for poration. Since the cells interact with the microbubbles, and not directly with the laser, the possibility of cell damage is reduced.

The setup of the LMP system is shown in Fig. 2. A fluidic chamber was formed by clamping a 1.1-mm-thick glass slide over the absorbent substrate, spaced by 20-µm-diameter polystyrene beads. A cell monolayer was pre-cultured on the bottom of the glass slide before the experiment. Microbubbles were generated by a 980-nm diode laser with a maximum power of 800 mW (Laserlands, 980MD-0.8W-BL). The laser was focused on the optically absorbent substrate through a 10x objective lens, and the measured intensity was 127 kW/cm^2 when the laser is on. The optically absorbent substrate consisted of a 1.1-mm-thick glass slide coated with a 200-nm-thick layer of indium tin oxide (ITO), topped by a 1-µm-thick layer of amorphous silicon (α-silicon). The majority of the incident light (70%) was absorbed in the ITO and α-silicon layers of the absorbent substrate [20] and converted into heat, creating microbubbles at the surface of the substrate. The laser pulse was controlled with a function generator (Agilent 33220A) to change pulse width and frequency, allowing control over the bubble size and oscillation speed.

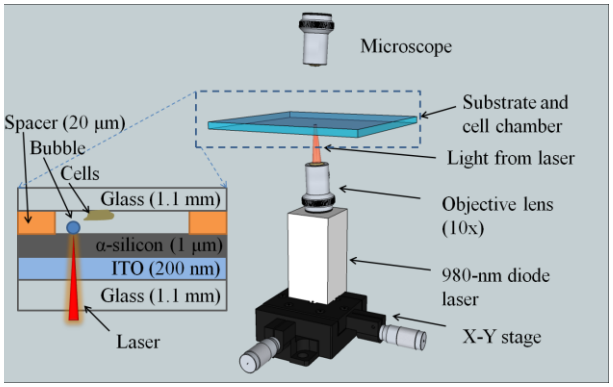

Figure 2. The light-induced microbubble poration (LMP) system. The microbubble is induced by a focused 980-nm diode laser. The optically absorbing substrate contains indium tin oxide (ITO) and amorphous silicon (α-silicon) layers. The cells are pre-cultured on a glass slide and sealed in the chamber.

III. Experimental Methods

A. Cell Preparation and Cell Viability Evaluation

The NIH/3T3 fibroblast cells were obtained from the ATCC. The cells were cultured on sterile glass slides using complete culture media consisting of Dulbecco's Modified Eagle's Medium (DMEM, from ATCC), 10% bovine serum (Gibco, Invitrogen), penicillin (100 U/ml), and streptomycin (100 µg/ml), in a humidified incubator at 37 °C and 5% CO_2. At the time of the experiments, the cells were sub-confluent.

Cell viability was assessed using Ethidium homodimer-1 (EthD-1) (Molecular Probes, Eugene, OR). This dye enters through damaged membranes and enhances fluorescence upon binding to nucleic acids, producing a bright red fluorescence in dead cells.

B. Molecular Delivery and Viability Assays

Fluorescein-isothiocyanate- (FITC) conjugated Dextran (Sigma-Aldrich, MW = 3 kDa) was used as a demonstration molecule for delivery. A solution of 5-mM FITC-Dextran in 1X phosphate buffered saline (PBS) was added to the cell chamber. After the microbubble poration process, the cells were incubated for 5 min, since the recovery time of the membrane is around 1 min [11]. A solution of 20-µM EthD-1 in complete culture media was used as a rinsing buffer to replace all the FITC-Dextran solution. The cells were incubated for another 20 min in the 20-µM EthD-1 solution before imaging under an Olympus BXFM fluorescent microscope.

C. LMP Parameters

The laser pulse width was in the range of 90 to 110 µs at a pulse frequency of 50 Hz. Under this test condition, the diameter of the bubbles is within the range of 7 to 10 µm. Longer laser pulse widths can increase the bubble size. The working distance between the edges of microbubble and cell to be porated was 2 µm or less. However, direct illumination of the cell by the laser was avoided. The laser pulses were activated for 15 s to obtain the poration results presented here. These LMP parameters were determined by empirical optimization of the poration efficiency and cell viability.

IV. Results and Discussion

A. Poration of Cell Monolayer

Sub-confluent NIH/3T3 cells were prepared as described in the previous section, and used to demonstrate the delivery of 3 kDa FITC-Dextran. Successful delivery was measured by observation under a fluorescent microscope. The poration efficiency and the cell viability can both reach 100% with careful control of the laser location. Eight of the cells in the field of view were subjected to the microbubble poration, followed by the cell viability assay. The bubble poration locations of the cell membrane were randomly chosen during the test. No difference was observed for poration occurring at various locations on the cell membrane. All eight porated cells maintained normal morphology after poration, as shown in the differential interference contrast (DIC) image (Fig. 3a). The porated cells displayed green fluorescence (Fig. 3b), indicating the successful delivery of FITC-Dextran. No red fluorescence was visible, indicating cell membrane integrity was restored, and that there was no cell death after poration.

B. Effect of Distance Between the Microbubble and the Cell

As mentioned earlier, the microbubble-induced shear stress should be carefully controlled. The shear stress should be gentle enough to avoid damaging the cells under poration and to avoid porating any neighboring cells, but still strong enough to porate cells near the bubble surface. The strength of

the shear stress at the cell membrane depends on the distance between the cell and the microbubble, making this an important parameter in the poration process.

To determine the optimum distance between the edges of the microbubble and the cell, poration tests were conducted at three different distances: the cell membrane in direct contact with the bubble, the cell membrane and bubble surface separated by a 5 µm gap, and the cell membrane and bubble surface separated by a 10 µm gap. The poration of several cells was attempted at each cell-bubble separation distance, followed by fluorescent imaging to detect the uptake of FITC-Dextran. Subsequently, the same cells underwent the EthD-1 viability assay. This was repeated two additional times, so that a total of at least 30 cells were measured at each separation distance. A total of 36 cells were tested in direct contact with the microbubble. At distances of 5 µm and 10 µm between the microbubble and cell, a total of 47 cells and 30 cells were measured, respectively.

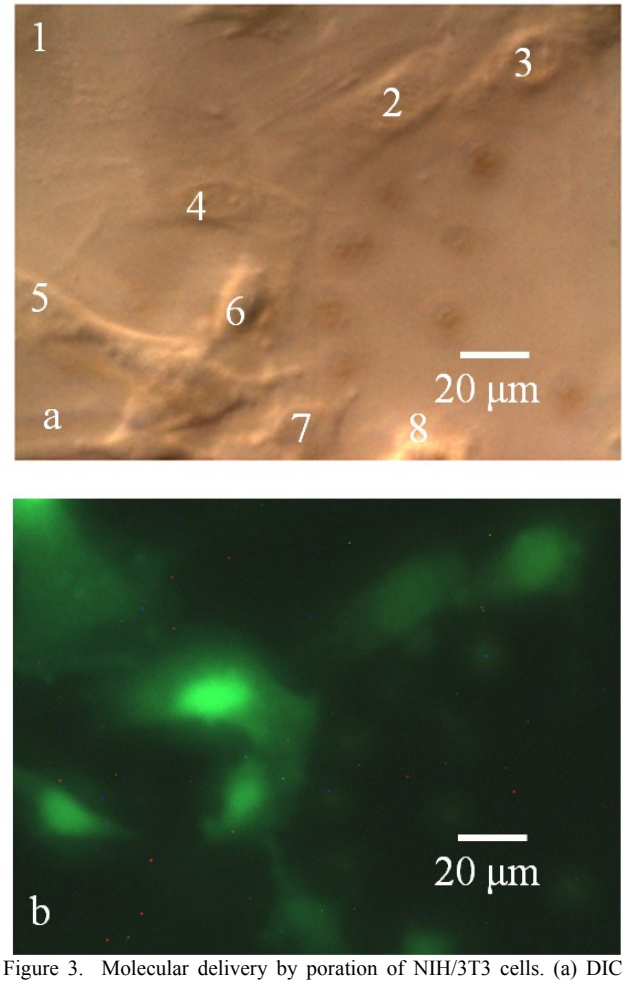

Figure 3. Molecular delivery by poration of NIH/3T3 cells. (a) DIC image of porated cells. (b) Fluorescent image of porated cells. All the processed cells were successfully porated, resulting in the delivery of 3-kDa FITC-Dextran, indicated by the green fluorescence. The cells did not display red fluorescence due to EthD-1, indicating that the cells were viable after poration.

As expected, the poration efficiency has a strong dependence on the distance between the cell and the microbubble (Fig. 4a). The poration efficiency was 95.2% ± 4.8% when the microbubble and cell directly contact each other. When the distance was increased, the poration efficiency decreased: it was 30.0% ± 5.0% at a distance of 5 µm, and 7.7% ± 3.9% at a distance of 10 µm. The cell viability for all these distances remained high (Fig. 4b). When the cell and microbubble directly contact each other, the cell viability was 97.6% ± 2.4%. For the longer distances of 5 µm and 10 µm, the cell viabilities were 100%.

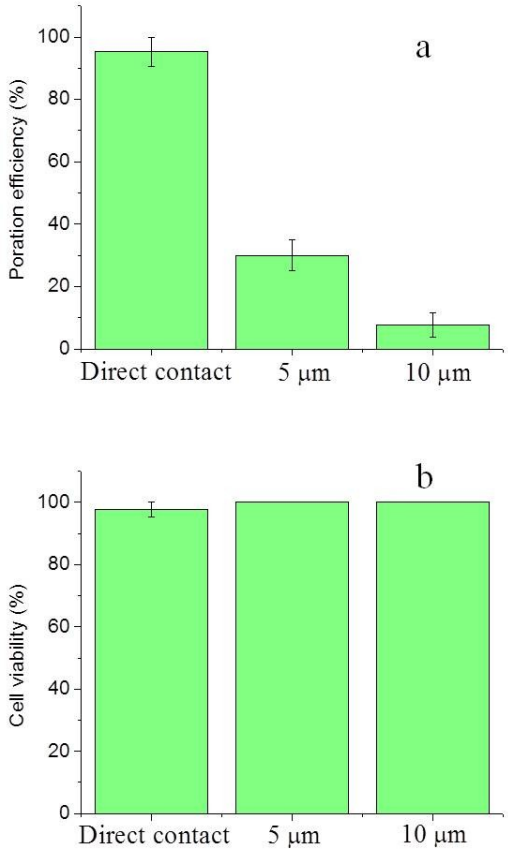

Figure 4. (a) Cell poration efficiency as a function of the distance between the microbubble and the cell membrane. Error bars show the standard error of the measurements. (b) Cell viability after poration.

C. Single-Cell Poration

As the control of the microbubble poration can be very precise, the LMP molecular delivery method has advantage of localized single-cell poration. Molecules can be delivered into only one target cell without affecting other neighboring cells (Fig. 5).

In this experiment, the cell monolayer was sub-confluent, so the spacing between neighboring cells was usually larger than 20 µm. As the poration efficiency using LMP decreases rapidly as distance between the microbubble and cell increases, neighboring cells were not porated. This enabled the poration of a single cell without affecting the state or viability of neighboring cells.

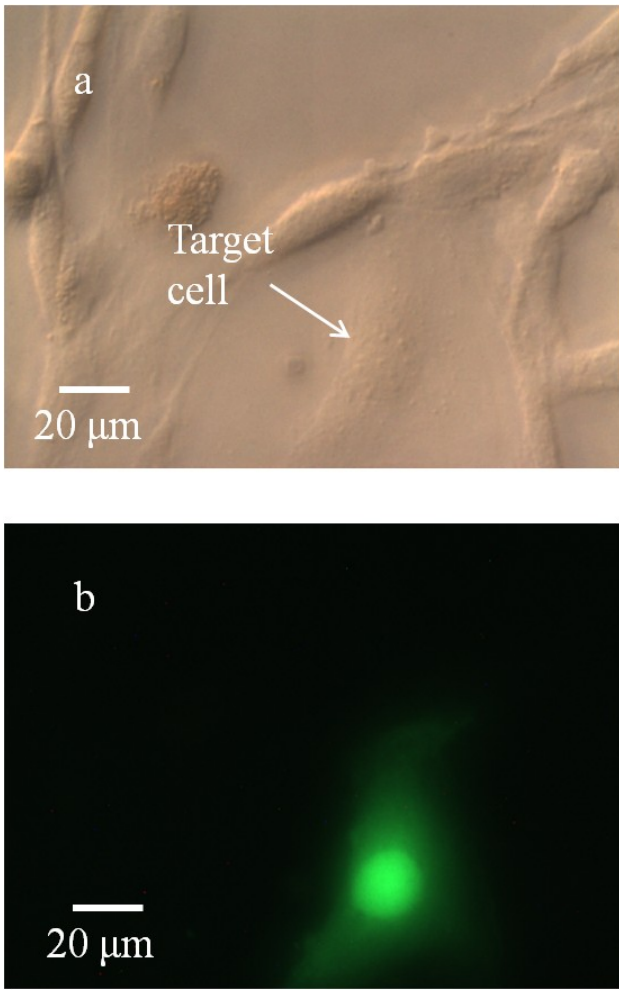

Figure 5. Single-cell poration result. (a) DIC image of cells after targeted single-cell poration. (b) Fluorescent image of porated target cell.

V. Conclusions and Future Work

Localized single-cell poration by laser-pulse-induced microbubbles was demonstrated and characterized. This molecular delivery method combines high-efficiency poration with a process that maintains high cell viability. The cell selectivity of this delivery method is also very high, as single cells in specific spatial locations can be porated. This addresses an area of need, as previous poration studies are more successful at addressing large groups of cells.

In the future, the parallel control of microbubbles can be achieved, enabling the poration of multiple target cells at the same time. A laser scanning system can project a single laser on multiple areas of the substrate within one period, as the laser pulse width (110 μs) is far smaller than the pulse period that was used (20 ms for a frequency of 50 Hz). Meanwhile, there is still potential space to reach higher poration efficiency with the improved control of the laser positioning.

References

[1] A. M. Bratt-Leal, *et al.*, "Engineering the embryoid body microenvironment to direct embryonic stem cell differentiation," *Biotechnology Progress,* vol. 25, pp. 43-51, Jan-Feb 2009.

[2] J. Wang, *et al.*, "The next step in gene delivery: molecular engineering of adeno-associated virus serotypes," *Journal of Molecular and Cellular Cardiology,* vol. 50, pp. 793-802, May 2011.

[3] A. M. Bodles-Brakhop, *et al.*, "Electroporation for the delivery of DNA-based vaccines and immunotherapeutics: current clinical developments," *Molecular Therapy,* vol. 17, pp. 585-592, Apr 2009.

[4] A. Valero, *et al.*, "Gene transfer and protein dynamics in stem cells using single cell electroporation in a microfluidic device," *Lab on a Chip,* vol. 8, pp. 62-67, Jan 2008.

[5] M. Y. Wang, *et al.*, "Single-cell electroporation," *Analytical and Bioanalytical Chemistry,* vol. 397, pp. 3235-3248, Aug 2010.

[6] J. K. Valley, *et al.*, "Parallel single-cell light-induced electroporation and dielectrophoretic manipulation," *Lab on a Chip,* vol. 9, pp. 1714-1720, Jun 2009.

[7] Y. Zhang, "Microinjection technique and protocol to single cells," *Nature Protocols,* http://dx.doi.org/10.1038/nprot.2007.487, Nov 2007.

[8] S.-W. Han, *et al.*, "High-efficiency DNA injection into a single human mesenchymal stem cell using a nanoneedle and atomic force microscopy," *Nanomedicine: Nanotechnology, Biology and Medicine,* vol. 4, pp. 215-225, Sept 2008.

[9] S. Mitragotri, "Healing sound: the use of ultrasound in drug delivery and other therapeutic applications," *Nature Reviews Drug Discovery,* vol. 4, p. 6, Mar 2005.

[10] Y. Qiu, *et al.*, "Microbubble-induced sonoporation involved in ultrasound-mediated DNA transfection in vitro at low acoustic pressures.," *Journal of Biomechanics,* vol. 45, pp. 1339-1345, May 2012.

[11] A. van Wamel, *et al.*, "Vibrating microbubbles poking individual cells: Drug transfer into cells via sonoporation," *Journal of Controlled Release,* vol. 112, pp. 149-155, May 2006.

[12] J. Wu, *et al.*, "Sonoporation, anti-cancer drug and antibody delivery using ultrasound," *Ultrasonics,* vol. 44, pp. E21-E25, Dec 2006.

[13] A. N. Hellman, *et al.*, "Biophysical response to pulsed laser microbeam-induced cell lysis and molecular delivery," *Journal of Biophotonics,* vol. 1, pp. 24-35, Feb 2008.

[14] T. H. Wu, *et al.*, "Photothermal nanoblade for large cargo delivery into mammalian cells," *Analytical Chemistry,* vol. 83, pp. 1321-1327, Feb 2011.

[15] U. K. Tirlapur and K. Konig, "Targeted transfection by femtosecond laser," *Nature,* vol. 418, pp. 290-291, Jul 2002.

[16] D. Stevenson, *et al.*, "Femtosecond optical transfection of cells: viability and efficiency," *Optics Express,* vol. 14, pp. 7125-7133, Aug 2006.

[17] J. Baumgart, *et al.*, "Quantified femtosecond laser based opto-perforation of living GFSHR-17 and MTH53a cells," *Optics Express,* vol. 16, pp. 3021-3031, Mar 2008.

[18] W. Hu, *et al.*, "Hydrogel microrobots actuated by optically generated vapour bubbles," *Lab on a Chip,* vol. 12, pp. 3821-3826, Oct 2012.

[19] K. R. Rau, *et al.*, "Pulsed laser microbeam-induced cell lysis: Time-resolved imaging and analysis of hydrodynamic effects," *Biophysical Journal,* vol. 91, pp. 317-329, Jul 2006.

[20] W. Hu, *et al.*, "Micro-assembly using optically controlled bubble microrobots in saline solution," *2012 IEEE International Conference on Robotics and Automation (ICRA),* pp. 733-738, May 2012.